Nematic-isotropic transition in a lattice model with quenched disordered impurities: A Monte Carlo study

Jaroslav Ilnytskyi* and Stefan Sokołowski
Department for the Modelling of Physico-Chemical Processes, Faculty of Chemistry, MSC University, 200-31 Lublin, Poland

Orest Pizio
Instituto de Quimica de la UNAM, Coyoacan 04510, Mexico, Distrito Federal, Mexico
(Received 12 November 1998)

We have performed Monte Carlo (MC) simulations of the lattice model for a fluid of elongated particles, mimicking liquid crystalline behavior and of this model in the presence of disordered quenched impurities. The interparticle interaction is chosen similar to the angular dependent term of the Berne-Pechukas potential. A pronounced first-order nematic-isotropic transition has been obtained for a bulk pure model at the value for the elongation parameter, $a=3$. However, at a 5% concentration of disordered quenched impurities, we have observed a very weak first-order transition in the simulations of the model at different sizes of the simulation volume. We have discussed a shift of the transition temperature, a suppression of the latent heat and the maxima of the heat capacity and susceptibility due to the presence of impurities. A histogram analysis and a finite-size scaling has been applied to the MC data. A comparison of the simulation data with the experimental results for liquid crystals confined to silica aerogels and porous glasses also has been performed.
[S1063-651X(99)09604-X]

PACS number(s): 61.30.Cz, 64.60.Cn, 02.70.Lq

I. INTRODUCTION

The structure, thermodynamics, and phase behavior of fluids confined to disordered porous media has received much attention during the past decade. A large body of experimental, simulational, and theoretical results has been accumulated. On the other hand, more interesting, and physically richer, complex fluids under confinement have received less attention. The liquid crystalline materials in confined geometry are of particular interest for basic science and for applied research.

Interest in liquid crystals (LCs) in the individual pores and in disordered porous media is very rapidly increasing, see, e.g., [1–16]. In particular, the nematic-isotropic (NI) transition in liquid crystals confined to microporous and mesoporous media has been studied experimentally [5–9]. The experimental results provide evidence that the finite size of pores, the effect of quenched disorder and the interconnectivity of pores, are main factors that influence phase behavior of LCs in microporous adsorbents. Theoretical investigation and simulation of the NI transition in porous media therefore must include modeling of the various factors crucial to the NI transition [10–16].

A set of numerical studies of liquid crystalline materials in microporous media has been attempted during the past decade. In particular, a model of trimers on a simple cubic (sc) lattice has been simulated by Dadmun and Muthukumar [12]. A porous medium has been implied as a dilution, i.e., it has been assumed that a fraction of sites of the lattice is inaccessible for trimers. The excluded volume effects of dilution have yielded a lower NI transition temperature and a rounder heat capacity maximum of the model, as compared to its pure counterpart. Moreover, the transition has been shown to change its nature from first to second order, if the concentration of impurities is larger than 2.5%. The simulation data have been shown to agree qualitatively with the experimental results. However, quantitatively the shift of the transition temperature compared to the pure model, i.e., in the absence of impurities, is essentially overestimated. It seems that the size of the lattice system considered in Ref. [12] (up to $16\times16\times16$ sites, such that the system consists of less than 1300 trimers) is insufficient to describe the thermodynamics quantitatively.

A study of the phase transitions in aerogel has been undertaken by Uzelac, Hasmy, and Jullian [13] in the framework of the $q=3$ and $q=4$ Potts models. The models are characterized by a weak first-order transition in the pure case. The aerogel has been modeled as a set of correlated impurities on the lattice by using diffusion-limited cluster-cluster aggregation; the case of randomly distributed impurities also has been studied in [13]. A finite-size scaling analysis (on the lattices up to 20^3 size) and the Ferrenberg-Swendsen (FS) histogram technique [17] have been used. The shift of the transition temperature with increasing concentration of impurities appeared to be smaller in the aerogel case, comparing with the case of randomly distributed impurities. The heat capacity peaks have been obtained as suppressed and essentially broadened with increasing impurity concentration. The finite-size scaling analysis of the simulation data has shown that the order of the transition for three-dimensional (3D) $q=3$ and $q=4$ Potts models changes at a nonzero concentration threshold. However, these results must be considered with some care due to the small lattice sizes involved, and due to the fact that systematic averages

*Permanent address: Institute for Condensed Matter Physics, National Academy of Sciences of Ukraine, 1 Svientsitskoho Str., UA-290011, Lviv, Ukraine. Electronic address: iln@icmp.lviv.ua

over disorder have not been performed. Nevertheless, the results presented in Ref. [13] confirm that even a weak dilution may essentially affect the NI transition (these trends were observed earlier by Hashim, Luckhurst, and Romano [18]).

Other models and theoretical developments concerning the behavior of liquid crystalline materials in the presence of quenched disorder have been proposed recently, in particular, the random-field Ising model [10,11], random anisotropy nematic model [15], and single-pore model for liquid crystal in aerogel [16].

In general, computer simulations are powerful tools for investigating the microscopic nature of the liquid crystalline phases. The most successfull intermolecular potentials applied in the simulations of the bulk models include the Berne-Pechukas [19] and Gay-Berne [20] potentials. However, reasonably large systems of molecules interacting via these potentials, appropriate to study phase transitions, are difficult to consider due to computer time consumption. Therefore, for practical reasons, it is important to obtain the simulation results for large systems of molecules in the framework of quite simple models, intrinsically preserving liquid crystalline nature.

With this aim, in the present study we perform Monte Carlo simulations of the NI transition in a modified Lebwohl-Lasher (LL) lattice model for liquid crystals [21], however, both in its pure state and in the presence of quenched random dilution. The particles in the model interact via the angular part of the Berne-Pechukas (BP) potential [19] derived from the overlap integral of two ellipsoidal Gaussians of a certain elongation a. The first-order NI transition in the pure modified LL model becomes stronger with increasing elongation parameter [21]. We consider the case $a=3$, that yields reasonable values for the latent heat and for the order parameter at the NI transition [21]. Our investigation of the model in the presence of a microporous media, is restricted to the case of a 5% dilution (which formally corresponds to a highly porous medium). A more ''liquid crystalline'' model is used in the present study, in comparison with previous works [12,13]. Consequently, the simulations are much more time consuming. Moreover, the lattice sizes up to 24^3 are simulated and a wide set of thermodynamical properties is discussed close to the NI transition. We would like to investigate how the dilution affects thermodynamic properties near the NI transition, and if the transition remains of the first order. On the other hand, our intention is to perform comparison with the available experimental results on LCs in highly porous confining media. A finite-size scaling analysis and the FS histogram technique [17] are used in the analysis of the simulation results.

II. NEMATIC-ISOTROPIC TRANSITION IN THE PURE MODEL

We consider a lattice model of elongated particles interacting via an angular part of the BP potential. The last one has the following form [19]:

$$V_{BP}(\hat{u}_i,\hat{u}_j,\vec{r}) = 4\epsilon(\hat{u}_i,\hat{u}_j) \times\left[\left(\frac{\sigma(\hat{u}_i,\hat{u}_j,\hat{r})}{r}\right)^{12}-\left(\frac{\sigma(\hat{u}_i,\hat{u}_j,\hat{r})}{r}\right)^{6}\right],$$

where $\epsilon(\hat{u}_i,\hat{u}_j)$ and $\sigma(\hat{u}_i,\hat{u}_j,\hat{r})$ are the effective orientationally dependent strength and range parameters, respectively. The unit vectors $\hat{u}_i,\hat{u}_j$ are directed along the corresponding long axes of the interacting ith, jth ellipsoids, $\vec{r}$ is the center-of-mass distance vector between them, and $\hat{r}$ is the unit vector along $\vec{r}$. In the case of rotators $\hat{u}_i$ on a lattice with the nearest-neighbors interaction only the angular dependence of $\epsilon(\hat{u}_i,\hat{u}_j)$,

$$\epsilon(\hat{u}_i,\hat{u}_j)=\frac{\epsilon_0}{\sqrt{1-\chi^2\cos^2\theta_{ij}}} \tag{1}$$

is involved (θ_{ij} is the angle between $\hat{u}_i$ and $\hat{u}_j$). The anisotropy of ellipsoids is characterized by the anisotropy parameter:

$$\chi=\frac{a^2-1}{a^2+1},\quad a=\frac{\sigma_\parallel}{\sigma_\perp},$$

where $\sigma_\parallel,\sigma_\perp$ are their major and minor axes, and a denotes the elongation parameter. In our computer simulations we use the following normalized interparticle interaction:

$$V_{BPA}(\theta_{ij})=-\frac{\epsilon}{2}\left[\frac{6a}{(a-1)^2}\left(\frac{1}{\sqrt{1-\chi^2\cos^2\theta_{ij}}}-1\right)-1\right], \tag{2}$$

where

$$\epsilon=\frac{(a-1)^2}{3a}\epsilon_0 \tag{3}$$

is the parameter used as energy unit in our simulations. For the sake of convenience, this potential is normalized such that at $\theta_{ij}=0$ and at $\theta_{ij}=\pi/2$ it gives the same energy (in units of ϵ) as the LL potential [22]. Moreover, the LL potential is reproduced in the limit of small anisotropy ($\chi \ll 1$) by expanding the expression given by Eq. 2 in powers of χ:

$$\lim_{\chi\ll 1} V_{BPA}(\theta_{ij})=-\epsilon P_2(\cos\theta_{ij})+\text{const.}$$

The first-order NI transition, that has been observed in the model at hand becomes stronger with the increasing elongation parameter a [21]. However, the parameter a provides only a rough estimate of the elongation of real molecules; it is more reasonable to think that the anisotropy of the intermolecular potential increases with augmenting value of the parameter a. On the other hand, stronger anisotropy can be achieved by adding higher P_{2n} terms to the LL potential [23–25] and choosing the expansion coefficients appropriately.

We restrict ourselves to the case $a=3$ in Eq. (2) [it is interesting to mention that in this case $V_{BPA}(\theta_{ij})$ coincides well with the potential considered by Romano [26] expanded up to P_6 term]. The value $a=3$ also has been used in the simulations of the Gay-Berne model [20].

We have performed simulations of the pure model with the potential $V_{BPA}(\theta_{ij})$ for four different lattice sizes

16^3,18^3,20^3,24^3 and apply a finite-size scaling analysis and the FS reweighting technique for the data obtained. Our principal interest is in the properties that are expected to change at a weak dilution. These are the transition temperature, the maximum values for the specific heat and susceptibility, the minima for the fourth Binder's cumulant, the latent heat and the order parameter at transition.

A numerical procedure for each lattice size was similar. First, short scanning runs (up to 10^5 MC cycles) were performed for the entire interval of temperatures including the NI transition point. Then we select a temperature for which a number of configurations (along the run), with predominant nematic or isotropic phase, is of the same order. A good indication for that is a regular ''flow'' of the order parameter values from about 0.05 to 0.3. At such a temperature, we would say, the coexistence of two phases is observed. Then, an extended run of the 5×10^5 MC cycles was performed at this temperature and the histograms of energy and of the order parameter have been built up. By applying the FS reweighting the NI transition point was located in the first approximation. This estimate for the NI transition temperature is used for the final extended run of not less than 10^6 MC cycles that provides final histograms and the quantities of interest.

A standard Metropolis algorithm has been used in our simulations. The orientation of each particle $\hat{u}_i$ was attempted to change by adding a vector $\vec{l}$ with random orientation and of controlled length [27], and then normalizing the value $\hat{u}_i' = \hat{u}_i + \vec{l}$ back to unity. A new configuration was accepted, if the energy becomes lower, or accepted with a Boltzmann probability otherwise. The length of $\vec{l}$ has been adjusted during simulation to provide a ratio of accepted attempts approximately equal to 0.4. The dimensionless temperature $T^* = k_B T/\epsilon$ is used in the simulations.

Each configuration is characterized by the one-particle energy

$$U^* = \frac{1}{N_f \epsilon} \sum_{ij} V_{BPA}(\theta_{ij})$$

(N_f is the number of unit vectors $\hat{u}_i$ in the simulation box) and the order parameter

$$S = \langle P_2(\cos\theta_i)\rangle_i ,$$

where θ_i is the angle between $\hat{u}_i$ and a director. The order parameter is calculated after each simulation cycle as the largest eigenvalue of the corresponding tensor [28].

The values of U^* and S have been stored after each MC cycle along the extended run performed at certain temperature T_0^*. These arrays were used to build up the normalized histograms of energy $P_{T_0^*}(U^*)$ and of the order parameter $P'_{T_0^*}(S)$ distribution at T_0^*. Using the method of Ferrenberg and Swendsen [17], the reweighted distributions $P_{T^*}(U^*)$ and $P'_{T^*}(S)$ have been obtained at each temperatute T^* in the vicinity of T_0^*. These distributions allow us to calculate the averages $\langle U^{*n}\rangle$ and $\langle S^n\rangle$ at each T^* in the vicinity of T_0^*, as well as dimensionless heat capacity, $C_v^* = C_v/(k_B N_f)$, and the susceptibility, $\chi^* = \chi\epsilon/N_f$, defined via the fluctuational formulas

$$C_v^* = \frac{N_f}{T^{*2}}(\langle U^{*2}\rangle - \langle U^*\rangle^2), \quad \chi^* = \frac{N_f}{T^*}(\langle S^2\rangle - \langle S\rangle^2).$$

Also, we have calculated the fourth Binder's cumulant of the energy fluctuations [29] as follows:

$$V_4 = 1 - \frac{\langle U^{*4}\rangle}{3\langle U^{*2}\rangle^2},$$

which is a useful additional estimate of the transition temperature, and serves to determine the order of the transition.

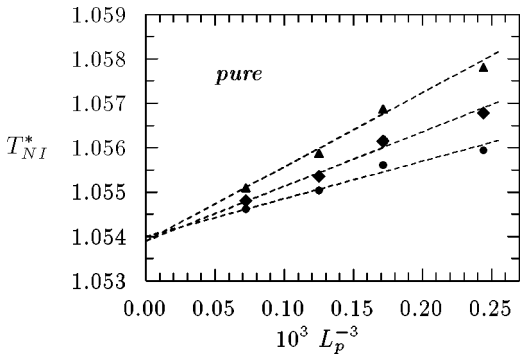

FIG. 1. Finite-size scaling behavior of the NI transition temperature in the pure model defined in different ways (circles and diamonds are obtained from the peaks of the heat capacity and the susceptibility, respectively; triangles are from the minima of the fourth Binder's cumulant), L_p is the linear size of the simulated model.

Let us denote the NI transition temperature (estimated in the framework of a procedure numbered by m) by $T^*_{m,NI}(L_p)$ for the system of L_p^3 size, p is the subscript introduced to emphasize the pure case. For the first-order transition, we would expect from Ref. [30] that $T^*_{m,NI}(L_p) - T^*_{m,NI}(\infty_p) \sim L_p^{-3}$, where $T^*_{m,NI}(\infty_p)$ is the transition temperature for an infinite system. Following Ref. [31] we have used three different procedures to evaluate the NI transition temperature for each system size. The locations of the peaks for $C_v^*(L_p)$ and $\chi^*(L_p)$ yield $T^*_{1,NI}(L_p)$ and $T^*_{2,NI}(L_p)$, respectively, and a location of the V_4 minimum gives $T^*_{3,NI}(L_p)$. The expected finite-size scaling behavior holds exactly for all $T^*_{m,NI}(L_p)$ (see, Fig. 1); this behavior is quite similar to the one observed for the LL model [31]. The fitting lines meet at $L_p^{-3} = 0$, giving the value

$$T^*_{NI}(\infty_p) = 1.0540 \pm 0.0002 \tag{4}$$

for an infinite system. We must mention that this value cannot be compared straightforwardly with the one for the LL model [31] due to a different energy scale [ϵ given by Eq. (3) is anisotropy dependent].

Another common test for the first-order transition is the scaling of the maxima for $C^*_{v\max}(L_p)$ and for $\chi^*_{\max}(L_p)$ proportionally to L_p^3, with increasing L_p. We have obtained typical rounded peaks for $C_v^*(L_p)$ and $\chi^*(L_p)$; both become

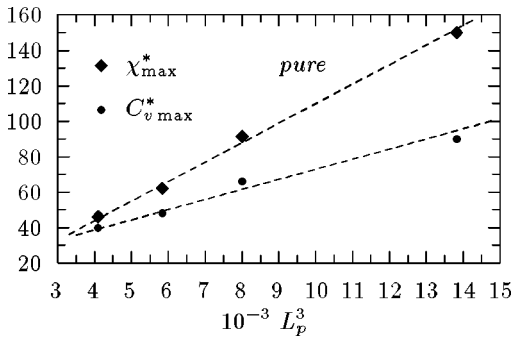

FIG. 2. Finite-size scaling behavior of the heat capacity $C^*_{v\max}$ and the susceptibility $\chi^*_{\max}$ maxima in the vicinity of the NI transition in the pure model of linear size L_p.

higher, narrower and shift to a lower value of T^* as L_p increases. For the sake of brevity, we do not present these curves in the present work (see, e.g. Refs. [13,31,32]). The values for $C_{v\max}(L_p)$ and for $\chi_{\max}(L_p)$ versus L_p^3, together with the corresponding fitting lines are shown in Fig. 2. One can see that the scaling law of the L_p^3 type is satisfied very well.

The properties that can be compared with the experiment are the latent heat at the NI transition $\Delta H_{NI}(L_p)$ and the order parameter $S_{NI}(L_p)$ at T_{NI}. To obtain the value for $\Delta H_{NI}(L_p)$ we seek first the temperature $T^*_{eq}(L_p)$, at which the maxima of the energy distribution $P_{T^*_{eq}}(U^*)$ are of equal height. This temperature turned out to be very close to the susceptibility peak position $T^*_{2,NI}(L_p)$ for all L_p. It is known that the energy distribution of a system close to the first-order transition can be approximated reasonably well by a double Gaussian [33]. However, we have obtained better fitting by using a double non-Gaussian distribution of the form

$$P_{T^*_{eq}}(U^*)\approx A_N \exp\left(-\frac{u_N^2}{\alpha_N}-\frac{u_N^3}{\beta_N}-\frac{u_N^4}{\gamma_N}\right) + A_I \exp\left(-\frac{u_I^2}{\alpha_I}-\frac{u_I^3}{\beta_I}-\frac{u_I^4}{\gamma_I}\right), \tag{5}$$

where $u_N = U^* - U^*_{nem}$ and $u_I = U^* - U^*_{iso}$ are the deviations of energy from the expected values U^*_{nem} and U^*_{iso} in nematic and isotropic phases, respectively. These expected values and the fitting coefficients are obtained numerically by using the least-squares method. The dimensionless latent heat per particle was then estimated at $T^*_{eq}(L_p)$ as $\Delta H^*_{NI}(L_p) = U^*_{iso} - U^*_{nem}$ (see Fig. 3). To get a better accuracy, we have used the following average: $\langle \Delta H^*_{NI}(L_p)\rangle_\pm = \frac{1}{3}[\Delta H^*_{NI}(L_p) + \Delta H^*_{NI+}(L_p) + \Delta H^*_{NI-}(L_p)]$, where $\Delta H^*_{NI+}(L_p)$ has been estimated similar to $\Delta H^*_{NI}(L_p)$ at $T^*_{eq}(L_p) + \delta T^*$ and $\Delta H^*_{NI-}(L_p)$ has been estimated at $T^*_{eq}(L_p) - \delta T^*$. Here (for the pure model) we choose $\delta T^* = 0.0005$. These estimates $\langle \Delta H^*_{NI}(L_p)\rangle_\pm$ do not exhibit a finite-size scaling dependence within the accuracy of our calculations (see, Fig. 4). The latent heat for an infinite system can be derived as the average over all simulated lattice sizes:

$$\Delta H^*_{NI}(\infty_p) = \langle\langle \Delta H^*_{NI}(L_p)\rangle_\pm\rangle_{L_p} = 0.179 \pm 0.005. \tag{6}$$

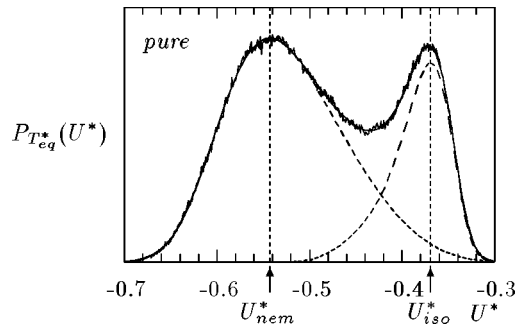

FIG. 3. Histogram of the energy distribution (the pure model, $L_p = 24$) at T^*_{eq} and its fit by a double non-Gaussian according to Eq. (5) (the fit practically coincides with the histogram). A nematic and an isotropic non-Gaussian also are shown separately. Their expected values are U^*_{nem} and U^*_{iso}, respectively.

Similar methodology has been used to evaluate the order parameter at the transition S_{NI}. In this case the distribution $P'_{T^*_{2,NI}}(S)$ is reweighted at $T^*_{2,NI}(L_p)$. The isotropic maximum, which is very low, was fitted by a Gaussian and the nematic maximum by a non-Gaussian:

$$P'_{T^*_{2,NI}}(S)\approx A'_N \exp\left(-\frac{s_N^2}{\alpha'_N}-\frac{s_N^3}{\beta'_N}-\frac{s_N^4}{\gamma'_N}\right) + A'_I \exp\left(-\frac{s_I^2}{\alpha'_I}\right), \tag{7}$$

where $s_N = S - S_{nem}$ and $s_I = S - S_{iso}$ (see, Fig. 5); moreover, we have assumed $S_{NI}(L_p) = S_{nem}$. Similar to the case of $\Delta H^*_{NI}(L_p)$, the averaging in the form $\langle S_{NI}(L_p)\rangle_\pm = \frac{1}{3}[S_{NI}(L_p) + S_{NI+}(L_p) + S_{NI-}(L_p)]$ has been used (the $+$ and $-$ signs have the same meanings as above). The values for $\langle S_{NI}(L_p)\rangle_\pm$ do not exhibit the L_p dependence within the statistical errors (see, Fig. 6). The average value over all simulated lattice sizes

$$S_{NI}(\infty_p) = \langle\langle S_{NI}(L_p)\rangle_\pm\rangle_{L_p} = 0.333 \pm 0.005 \tag{8}$$

is used as an estimate for an infinite system. The results obtained for the latent heat and for the order parameter are more accurate in comparison with our previous study [21], in

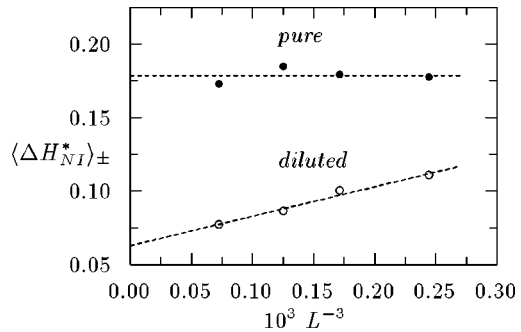

FIG. 4. Finite-size scaling behavior of the latent heat of the NI transition calculated as $U^*_{iso} - U^*_{nem}$ and averaged over the vicinity of T^*_{eq}. Black circles represent the pure model, the average is shown by the dashed line. Empty circles are for the diluted model, a dashed line corresponds to the linear fit.

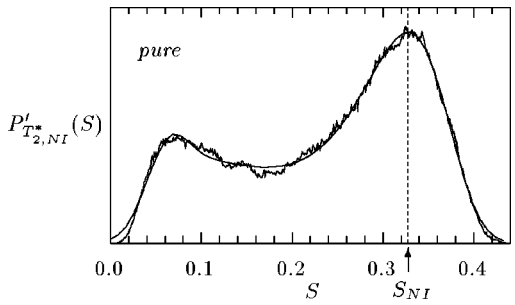

FIG. 5. Histogram of the order parameter distribution (the pure model, $L_p=24$) at the temperature $T^*_{2,NI}$ and its fit by a sum of a Gaussian and a non-Gaussian according to Eq. (7). The expected value of a nematic non-Gaussian gives the order parameter at the transition, S_{NI}.

which a system of single size has been simulated, and in which the FS technique has not been applied to the simulation data.

To conclude this section, the pure model undergoes a pronounced first-order NI transition. This conclusion follows from a finite-size behavior of the transition temperature, heat capacity, and susceptibility. The latent heat and the order parameter at the transition are obtained by fitting the corresponding histograms. These properties are of particular interest. We would like to compare them with a weakly diluted case, which is the subject of the following section.

III. NEMATIC-ISOTROPIC TRANSITION IN A WEAKLY DILUTE MODEL

The method described above is now applied to study a weakly dilute model. We have used a so-called random dilution, i.e., when N_m randomly chosen lattice sites are assumed to be occupied by quenched impurities. The other sites, $N_f=N-N_m$, are characterized by the unit vectors $\hat{u}_i$, which describe the orientational interactions between liquid crystal molecules. Similar to the pure model, a nearest-neighbors interaction between $\hat{u}_i$ and $\hat{u}_j$ is assumed, also we assume that there is no interaction between the impurities and $\hat{u}_i$. Therefore, only the effects of excluded volume are taken into account. A porous medium formed by impurities

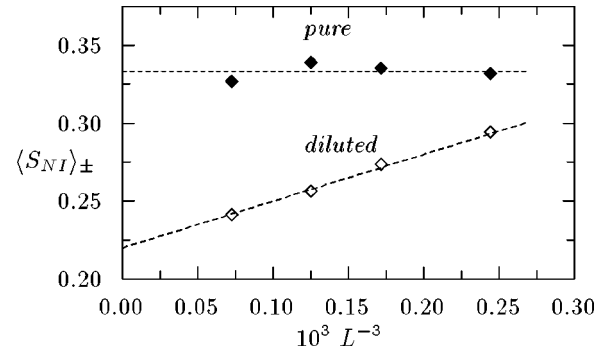

FIG. 6. Finite-size scaling behavior of the order parameter at the NI transition obtained from the fits at $T^*_{2,NI}$ and averaged over the vicinity at this temperature. Black diamonds represent the pure model, the average is shown as the dashed line. Empty diamonds are for the diluted model, the dashed line is a linear fit.

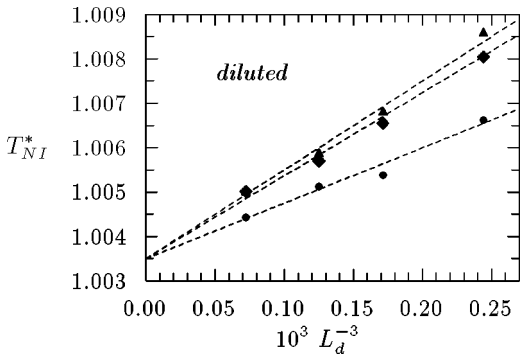

FIG. 7. Finite-size scaling behavior of the NI transition temperature in the diluted model defined in different ways (the meaning of the symbols is the same as in Fig. 1), L_d is the linear size of the simulated system.

may be thought to consists of highly interconnected pores. We consider the case of a weak dilution, $c=N_m/N=0.05$, which may correspond to a LC confined in a highly porous medium. Due to the CPU time limitations, we have averaged the results over not more than three quenched configurations of impurities for each lattice size.

Similar to the pure model, we denote the NI transition temperature of the dilute model of linear size L_d estimated in the framework of a procedure denoted by m by $T^*_{m,NI}(L_d)$. An estimate for the NI transition temperature from the peak for $C^*_v(L_d)$ and for $\chi^*(L_d)$ corresponds to $m=1,2$, respectively, and from the minimum of V_4 corresponds to $m=3$. We have observed the shift of the transition temperature of the order $[T^*_{m,NI}(L_p)-T^*_{m,NI}(L_d)]/T^*_{m,NI}(L_p)\approx c=0.05$ for each lattice size in accordance with a mean field estimate. A finite-size scaling behavior for the first-order transition, $T^*_{m,NI}(L_d)-T^*_{m,NI}(\infty_d)\sim L_d^{-3}$, holds very well within the accuracy of our data (see, Fig. 7). For an infinite system, we obtain

$$T^*_{NI}(\infty_d)=1.0035\pm 0.0002. \tag{9}$$

Further confirmation of the first-order nature of the transition in the dilute model is the finite-size scaling behavior of the maxima $C^*_{v\max}(L_d)$ and $\chi^*_{\max}(L_d)$. The heights of the maxima are essentially supressed, compared with the pure model. But their L_d^3 dependence expected for the first-order transition is still pronounced (Fig. 8).

The presence of dilution has a strong effect on the form of the energy and order parameter distributions $P_{T*}(U^*)$ and

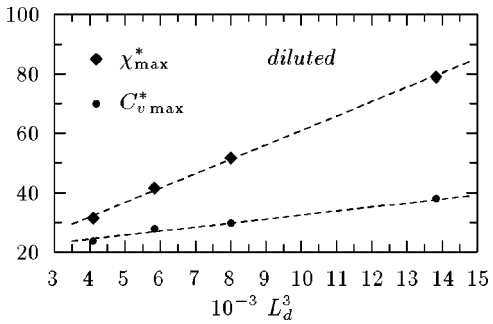

FIG. 8. Finite-size scaling behavior of the heat capacity $C^*_{v\max}$ and the susceptibility $\chi^*_{\max}$ maxima in the vicinity of the NI transition in the diluted model of linear size L_d.

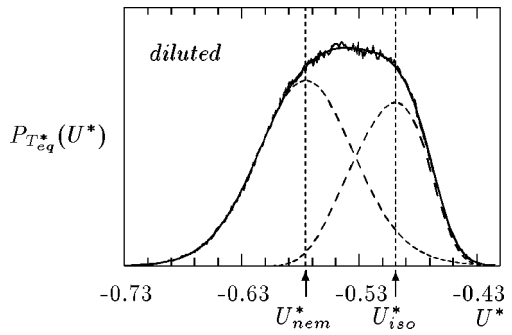

FIG. 9. Histogram of the energy distribution (the diluted model, $L_d=24$) at T^*_{eq} and its fit by a double non-Gaussian according to Eq. (5). A nematic and an isotropic non-Gaussian also are shown separately. Their expected values are U^*_{nem} and U^*_{iso}, respectively.

$P'_{T^*}(S)$. Even for the largest lattice size simulated, $L=24$, the double-maxima form for the energy distribution is not observed. This is due to a much weaker first-order transition. The distributions for two coexisting phases intersect essentially and it is practically impossible to evaluate the spinodal points for this case. Therefore, we are not able to define formally the temperature T^*_{eq}, with equally heighted maxima (as for the pure model). Instead, we have used the temperature where the upper part of the distribution has a symmetric shape (see, Fig. 9). Similar fitting formula for $P_{T^*}(U^*)$ (5) was used to extract the expected values for U^*_{nem} and U^*_{iso}, and to estimate a latent heat of the transition $\Delta H^*_{NI}(L_d) = U^*_{iso} - U^*_{nem}$ (see Fig. 9). We have observed that this procedure is very sensitive to the accuracy of the distribution tails. The accuracy can be unsufficient for the simulated temperature farther from T^*_{eq}. In this case, an additional curvature of the distribution tails is present, and the least-squares method fails to fit the histograms correctly. Similar to the pure case, we have calculated the average $\langle \Delta H^*_{NI}(L_d)\rangle_{\pm} = \frac{1}{3}[\Delta H^*_{NI}(L_d) + \Delta H^*_{NI+}(L_d) + \Delta H^*_{NI-}(L_d)]$ for each L_d, where $\Delta H^*_{NI+}(L_d)$ has been estimated at $T^*_{eq}(L_d) + \delta T^*$ and correspondingly the value for $\Delta H^*_{NI-}(L_d)$ at temperature $T^*_{eq}(L_d) - \delta T^*$. The shift of the temperature, $\delta T^* = 0.000\,25$, was chosen twice smaller, in comparison with the pure model. At these shifted temperatures, $T^*_{eq}(L_d) \pm \delta T^*$, the distribution is essentially asymmetric with the isotropic or nematic maxima clearly seen. Therefore a value, $\Delta H^{+}(L_d) = U^*_{iso}(T^*_{eq} + \delta T^*) - U^*_{nem}(T^*_{eq} - \delta T^*)$, provides a reasonable upper limit of the latent heat. In the majority of cases it is approximately 10% higher than the value $\langle \Delta H^*_{NI}(L_d)\rangle_{\pm}$. We have used this fact as an additional test. As one can see in Fig. 4, the values for $\langle \Delta H^*_{NI}(L_d)\rangle_{\pm}$ reflect the L_d dependence. For an infinite system we then obtain the value

$$\Delta H^*_{NI}(\infty_d) = 0.063 \pm 0.002, \tag{10}$$

which is essentially lower, if compared with 0.179 for the pure model (6).

The order parameter at the transition is estimated quite similar to the pure model. The only difference is that at $T^*_{2,NI}(L_p) + \delta T^*$, the nematic maximum for the order parameter is not very well defined to provide fitting successfully. Thus, instead of evaluating the average, $\langle S_{NI}(L_d)\rangle_{\pm}$, we have investigated the dependence of $S_{NI-}(L_d)$ [obtained from the fitting at temperature $T^*_{2,NI}(L_d) - \delta T^*$, slightly lower than $T^*_{2,NI}(L_d)$] with increasing δT^*. One might expect linear dependence on δT^*, if it is chosen small. This is indeed the case for $\delta T^* \in [0.000\,25, 0.000\,75]$. We have used this fact as an additional test of stability of the fit at $T^*_{2,NI}(L_d)$. One can note a well pronounced L_d dependence of $S_{NI}(L_d)$ (see, Fig. 6), in contrast to the pure model. Thus, the fitting procedure yields for an infinite system the value

$$S_{NI}(\infty_d) = 0.220 \pm 0.005. \tag{11}$$

This value must be compared with the value 0.333 for the pure model (8).

The essential finite-size dependence of the latent heat and of the order parameter for the diluted model can be explained according to the following arguments. The finite-size behavior of the pure system is governed by the fact that the correlation lenght ξ cannot overcome linear size of the system, L. Therefore, in the pure model all of the singularities are scaled by the single characterictic length ξ [30]. In the dilute model, another characteristic length appears, which is an average distance between impurities. Alternatively, influence of the dilution on the phase transition can be described by the parameter $\kappa = c\xi^3$ (proposed by Imry and Wortis [34]), κ represents the average number of impurities in a coherence volume. Actually, this parameter measures the relative influence of impurities on the phase transition. We assume that this parameter must be kept constant for different L, rather than the absolute concentration of impurities c. For $L < \xi_{bulk}$, one can assume that $\xi_L \approx L$, therefore it seems reasonable to keep constant the parameter $\kappa = cL^3$ for different L. Thus, in this case, one must rescale c by L^{-3} with increasing L. For L larger than ξ_{bulk}, a concentration corresponding to saturation, c_{bulk}, would arise. This concentration characterizes a diluted system of infinite size. In the case of a constant dilution, used most generally, one would obtain a progressive suppression of the transition by impurities as L increases (this behavior can be seen from Figs. 4 and 6).

To summarize the results about the influence of a constant, weak, 5% dilution on the NI transition in the lattice model of this study we would like to mention the following. At chosen concentration of impurities, the transition remains the first-order transition. However, it is much weaker than for the pure case, i.e., in the absence of impurities. A shift of the transition temperature in an infinite system according to Eqs. (4) and (9) can be written in the form of a ratio:

$$\frac{T^*_{NI}(\infty_d)}{T^*_{NI}(\infty_p)} = 0.952 \pm 0.0004. \tag{12}$$

The supression of the maxima of the heat capacity and of the susceptibility in an infinite system can be obtained from a fit using finite-size data (see Fig. 10). We have obtained the following ratios:

$$\frac{C^*_{v\max}(\infty_d)}{C^*_{v\max}(\infty_p)} = 0.35 \pm 0.01, \quad \frac{\chi^*_{\max}(\infty_d)}{\chi^*_{\max}(\infty_d)} = 0.45 \pm 0.01. \tag{13}$$

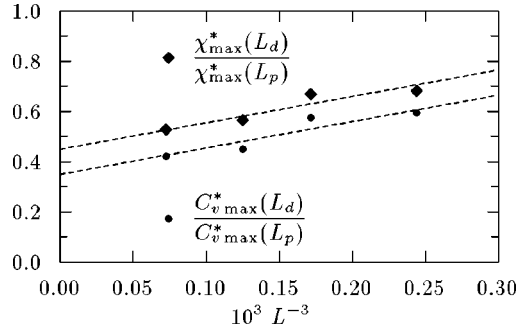

FIG. 10. Suppress of the heat capacity $C^*_{v\max}$ and the susceptibility $\chi^*_{\max}$ maxima resulting from a dilution of the model. Here $L_p=L_d=L$ and indices d and p denote the pure and diluted model, respectively.

A decrease of the latent heat and of the order parameter at the transition point in an infinite system are obtained by using the values (6,8,10,11). Then, our estimates are,

$$\frac{\Delta H^*_{NI}(\infty_d)}{\Delta H^*_{NI}(\infty_p)}=0.35\pm 0.02, \quad \frac{S_{NI}(\infty_d)}{S_{NI}(\infty_p)}=0.66\pm 0.02. \tag{14}$$

It must be mentioned that the effects of lowering the transition temperature, and of suppression of the heat capacity maxima, have been observed previously for a dilute model of trimers undergoing orientational transition [12], for $q=3,4$ state dilute Potts models [13], and for the model of random anisotropy [15]. However, in the present study we have simulated a quite different model and studied the influence of dilution on the susceptibility, on the latent heat and on the order parameter.

IV. COMPARISON WITH EXPERIMENTAL RESULTS

The influence of dilution on thermodynamic properties close to the NI transition can be related to the experimental results for LC's confined in a highly porous media. In particular, Wu *et al.* [9] have studied the NI transition in 8CB LC confined to silica aerogels at different porosity. For $\rho=0.08\ \mathrm{g\,cm^{-3}}$ aerogel density (which corresponds roughly to the 5% volume fraction of impurities for our model) the shift of T_{NI} of the magnitude $-0.45°$ has been observed, thus yielding $T^{gel}_{NI}/T^{pure}_{NI}=0.9986$. The shift, following from our simulations, and given by the ratio (12) is much more pronounced. The integrated enthalpy estimated from the experiment is given by $\delta H=\Delta H+\delta W$, where ΔH is the latent heat and δW is the contribution from the integrated area of a pretransitional region. For the pure model, it follows that $\delta H_{pure}=\Delta H_{pure}+\delta W=(2.1+5.58)\ \mathrm{J\,g^{-1}}$ [9]. It was observed experimentally, that the heat capacity points (plotted versus temperature) for aerogels at different density may be fitted by the same curve in the ''pretransitional'' region (except for the area of approximately 1.5° width near the transition point) [9]. This lead to the assumption that the density of a confining aerogel influences mostly the value for ΔH, but do not affect strongly the values for δW. In this case, one can use the ratio $\Delta H_{dil}/\Delta H_{pur}=0.35$ [Eq. (14)] from the simulations and obtain an estimate, $\delta H_{dil}=\Delta H_{dil}+\delta W=(0.735+5.58)\mathrm{J\,g^{-1}}=6.315\mathrm{J\,g^{-1}}$. This value is indeed very close to the experimental one, $\delta H_{gel}=6.28\ \mathrm{J\,g^{-1}}$, for $\rho=0.08\ \mathrm{g\,cm^{-3}}$ aerogel [9]. We can also compare the suppression of the heat capacity maxima by increasing progressively the aerogel density ρ. As it follows from the experiment [9], the excess heat capacity $\Delta C_{p\max}$ decreases almost linearly with the increasing ρ, at $\rho<0.36\ \mathrm{g\,cm^{-3}}$. For the aerogel densities, $\rho_1=0.08\ \mathrm{g\,cm^{-3}}$ and $\rho_2=0.17\ \mathrm{g\,cm^{-3}}$, we then obtain the ratio $\Delta C_{p\max}(\rho_2)/\Delta C_{p\max}(\rho_1)=0.51$, which is higher, but nevertheless comparable to the ratio 0.35 [Eq. (13)] obtained in the simulations.

Other experiments for the NI transition in 8CB LC confined to porous glasses have been performed by Iannacchione *et al.* [8]. In the case of a macroporous confinement (1000 Å mean pore size), the shift of the transition temperature of $-2.05°$ has been observed. This gives a ratio $T^{glass}_{NI}/T^{pure}_{NI}=0.993$ which again is higher than the ratio (12). The latent heat ΔH_{glass} has been shown to decrease and the ratio $\Delta H_{glass}/\Delta H_{pur}$ is 0.74; it is approximately twice as large as Eq. (14). Similar discrepancy can be observed for the suppression of the heat capacity, $\Delta C_{p\max}(glass)/\Delta C_{p\max}(pure)=0.65$, which is again higher than 0.35 [Eq. (13)]. In this context, it is interesting to note that the values obtained for the smallest lattice, $L_d=16$, are much closer to the experimental data, giving $\Delta H^*_{NI}(16_d)/\Delta H^*_{NI}(16_p)=0.63$ and $C^*_{v\max}(16_d)/C^*_{v\max}(16_p)=0.60$. Augmenting discrepancy with increasing system size is due to the hypothesis that the dilution concentration, c, must be rescaled for a finite-size system, keeping the value $c\xi^3$ constant.

We have obtained an essential overestimate for the suppression of the NI transition at a weak 5% dilution, when compared with the experiments. However, our results have been obtained in an infinite volume limit via finite-size scaling. Following the considerations of Imry and Wortis [34], we had assumed that the value $c\xi^3$ must be kept constant at increasing L, rather than the impurity concentration c. Nevertheless, a shift of the transition temperature is overestimated. Possible explanation of these trends is that one particle in a lattice model describes a group of real molecules, rather than a single one (a simple estimate of Bellini *et al.* [16] has shown that a group of approximately ten molecules corresponds to a site in the LL model). Thus, a dilution due to only one site would destroy six bonds on the sc lattice, and the energy of six surrounding particles (six groups of molecules) would be essentially underestimated. The temperature of the transition, in fact, is proportional to the number of ''surviving'' bonds, so it would shift too much. According to that argument, we would like to mention, in particular, that a 5% dilution corresponds effectively to a higher density aerogel than the $\rho=0.08\ \mathrm{g\,cm^{-3}}$ implied in a comparison performed above.

V. CONCLUSIONS

We have performed extensive Monte Carlo simulations of a weakly dilute liquid crystal lattice model with quenched impurities. The nearest neighbors interact via the angular part of the Berne-Pechukas potential. The elongation parameter is chosen equal to 3; the corresponding pure system undergoes a pronounced first-order nematic-isotropic transi-

tion. The model in the presence of impurities at a constant dilution of 5% has been simulated; four lattice sizes with linear dimensions $L=16,18,20,24$ have been used. The results of simulations have been averaged over three quenched configurations of impurities for each lattice size. The Ferrenberg-Swendsen reweighting technique has been used in the vicinity of the transition; also, a finite-size scaling analysis was applied to the simulation data. The latent heat of the transition and the order parameter have been evaluated by fitting the correspondent histograms by a double non-Gaussian distribution.

We have observed an essential suppression of the nematic-isotropic transition in the model at 5% dilution. This result is in agreement with general theoretical estimates of the influence of the quenched disorder on the first-order transitions [35,36]. However, at a 5% dilution considered here, the nematic-isotropic transition remains an extremely weak first order. A shift of the transition temperature, a suppression of the latent heat and of the heat capacity maxima in the infinite volume limit have been obtained. However, these effects are essentially overestimated, in comparison with the experiments on the 8CB liquid crystal confined to a highly porous media. This behavior seems to appear due to the assumption of rescaled concentration of dilutions for a finite system at a fixed value for the parameter $c\xi^3$.

ACKNOWLEDGMENTS

This work has been supported in parts by the State Fund for Fundamental Investigations under Program No. DKNT 2.4/173 of the Ukrainian State Commitee for Science and Technology, by the National Committee for Science and Technology (CONACyT) of Mexico under Grant No. 25301-E, and by the National University of Mexico (Project No. DGAPA-IN 111597). One of us (J.I.) is indebted to G. R. Luckhurst, S. Romano, C. Zannoni, and M. P. Allen for very stimulating discussions during the NATO ASI ''Advances in the Computer Simulation of Liquid Crystals,'' Erice.

[1] *Liquid Crystals in Complex Geometries Formed by Polymer and Porous Networks*, edited by G. P. Crawford and S. Žumer (Taylor and Francis, London, 1996).
[2] B. Jérôme, Rep. Prog. Phys. **54**, 391 (1991).
[3] G. S. Iannacchione and D. Finotello, Phys. Rev. Lett. **69**, 2094 (1992).
[4] G. P. Crawford and J. W. Doane, Condens. Matter News **1**, 5 (1992).
[5] M. D. Dadmun and M. Muthukumar, J. Chem. Phys. **98**, 4850 (1993).
[6] T. Bellini, N. A. Clark, C. D. Muzny, L. Wu, C. W. Garland, D. W. Schaefer, and B. J. Oliver, Phys. Rev. Lett. **69**, 788 (1992).
[7] G. S. Iannacchione, G. P. Crawford, S. Qian, J. W. Doane, D. Finotello, and S. Žumer, Phys. Rev. E **53**, 2402 (1996).
[8] G. S. Iannacchione, S. Qian, D. Finotello, and F. M. Aliev, Phys. Rev. E **56**, 554 (1997).
[9] L. Wu, B. Zhou, C. W. Garland, T. Bellini, and D. W. Schaefer, Phys. Rev. E **51**, 2157 (1995).
[10] M. J. P. Gingras (unpublished).
[11] A. Maritan, M. Cieplak, T. Bellini, and J. R. Banavar, Phys. Rev. Lett. **72**, 4113 (1994).
[12] M. D. Dadmun and M. Muthukumar, J. Chem. Phys. **97**, 578 (1992).
[13] K. Uzelac, A. Hasmy, and R. Jullien, Phys. Rev. Lett. **74**, 422 (1995).
[14] A. Maritan, M. Cieplak, and R. Banavar, in *Liquid Crystals in Complex Geometries Formed by Polymer and Porous Networks*, edited by G. P. Crawford and S. Žumer (Taylor and Francis, 1996), p. 483.
[15] D. J. Cleaver, S. Kralj, T. J. Sluckin, and M. P. Allen, in *Liquid Crystals in Complex Geometries Formed by Polymer and Porous Networks*, edited by G. P. Crawford and S. Žumer (Taylor and Francis, London, 1996), p. 467.
[16] T. Bellini, C. Chiccoli, P. Pasini, and C. Zannoni, Phys. Rev. E **54**, 2647 (1996).
[17] A. M. Ferrenberg and R. H. Swendsen, Phys. Rev. Lett. **61**, 2635 (1988).
[18] R. Hashim, G. R. Luckhurst, and S. Romano, Liq. Cryst. **1**, 133 (1986).
[19] B. J. Berne and P. Pechukas, J. Chem. Phys. **56**, 4213 (1972).
[20] J. G. Gay and B. J. Berne, J. Chem. Phys. **74**, 3316 (1981).
[21] Ja. M. Ilnytskyi, J. Phys. Stud. **1**, 232 (1997); Mol. Cryst. Liq. Cryst. **323**, 113 (1998).
[22] P. A. Lebwohl and G. Lasher, Phys. Rev. A **6**, 426 (1972).
[23] C. Chiccoli, P. Pasini, F. Biscarini, and C. Zannoni, Mol. Phys. **65**, 1505 (1988).
[24] G. I. Fuller, G. R. Luckhurst, and C. Zannoni, Chem. Phys. **92**, 105 (1985).
[25] S. Romano, Liq. Cryst. **16**, 1015 (1994).
[26] S. Romano, Int. J. Mod. Phys. B **9**, 85 (1995).
[27] R. Eppenga and D. Frenkel, Mol. Phys. **52**, 1303 (1984).
[28] J. Vieillard-Baron, Mol. Phys. **28**, 809 (1974).
[29] K. Binder, Z. Phys. B **43**, 119 (1981).
[30] K. Binder, Rep. Prog. Phys. **50**, 783 (1987).
[31] Zh. Zhang, O. G. Mouritsen, and M. J. Zuckermann, Phys. Rev. Lett. **69**, 2803 (1992).
[32] D. J. Cleaver and M. P. Allen, Mol. Phys. **80**, 253 (1993).
[33] M. S. S. Challa, D. P. Landau, and K. Binder, Phys. Rev. B **34**, 1841 (1986).
[34] Y. Imry and M. Wortis, Phys. Rev. B **19**, 3580 (1979).
[35] A. N. Berker, Bull. Am. Phys. Soc. **14**, 1990 (1990).
[36] J. Cardy, in *Book of Abstracts of the XXth IUPAP International Conference on Statistical Physics*, Paris, 1998, edited by A. Gervois, M. Gingold, and D. Iagolnitzer (UNESCO, Sorbonne, 1998), T1680: IL04/4.